Soft Matter

PAPER

View Article Online
View Journal | View Issue

Check for updates

Cite this: *Soft Matter*, 2026, **22**, 212

Radical scaling: beyond our feet and fingers

M. A. Fardin, †*[a] M. Hautefeuille [b] and V. Sharma †[c]

Received 30th September 2025,
Accepted 21st November 2025

DOI: 10.1039/d5sm00996k

rsc.li/soft-matter-journal

Scaling laws arise and are eulogized across disciplines from natural to social sciences for providing pithy, quantitative, 'scale-free', and 'universal' power law relationships between two variables. On a log–log plot, the power laws display as straight lines, with a slope set by the exponent of the scaling law. In practice, a scaling relationship works only for a limited range, bookended by crossovers to other scaling laws. Leading with Taylor's oft-cited scaling law for the blast radius of an explosion against time, and by collating an unprecedented amount of datasets for laser-induced, chemical and nuclear explosions, we show distinct kinematics arise at the early and late stages. We illustrate that picking objective scales for the two axes using the transitions between regimes leads to the collapse of the data for the two regimes and their crossover, but the third regime is typically not mapped to the master curve. The objective scales permit us to abandon the arbitrarily chosen anthropocentric units of measurement, like feet for length and heart-beat for time, but the decimal system with ten digits (fingers) is still part of the picture. We show a remarkable collapse of all three regimes onto a common master curve occurs if we replace the base 10 by a dimensionless radix that combines the scales from the two crossovers. We also illustrate this approach of radical scaling for capillarity-driven pinching, coalescence and spreading of drops and bubbles, expecting such generalizations will be made for datasets across many disciplines.

Published on 21 November 2025. Downloaded on 2/9/2026 5:09:59 PM.

Scaling laws expressed in arbitrary units often fail when observations span a broader range. Transitions between regimes reveal objective units, allowing to capture these regimes and their crossovers. Beyond units, we must reconsider the numerical base (radix) we use. Decimal, derived from our ten fingers, dominates, but natural phenomena operate independently of human conventions. By analyzing transitions between successive scaling regimes, we propose using a number derived from the system itself as the base instead of 10. This approach captures universal behavior across regimes, creating new opportunities to revisit examples from diverse disciplines. Such a framework challenges anthropocentric standards, offering deeper insight into how numbers and units emerge directly from physical phenomena.

What we see, perceive, and measure in the natural world is the combination of what is, and the angle, perspective, or reference frame we have chosen. Finding out what this elusive thing *is* then requires an array of viewpoints to overlap. For the practitioners of scaling analysis this overlap is understood quite literally. One may initially start with a messy set of intersecting data sets, and then strive to find the "right scale" with which the data almost magically overlap. Usually this quest stops when one finds judicious units for both axes of the plot. In this contribution, we show that a more complete scaling analysis should seek not solely to find units, but also to renormalize the very base we use for counting. Conventionally the base is 10, like the number of our fingers. However, fingers are no more legitimate than feet to count and measure.

The starting point of a scaling analysis is usually a scaling law or power law, *i.e.* a relation of proportionality between one variable and some power of another, $y = Kx^{\alpha}$.[1,2] Relationships of this kind are found everywhere. The periods of rotation of a planet is proportional to its distance to the Sun raised to a power $\alpha = \frac{3}{2}$ (Kepler law). The mean square displacement of a diffusive particle is proportional to the square root of the time, so with $\alpha = \frac{1}{2}$ (Einstein–Smoluchowski law). The metabolic rate of many animals is proportional to their mass to the power $\alpha = \frac{3}{4}$ (Kleiber law). The forces of gravity or of electrostatics are inversely proportional to the square of the distance, $\alpha = -2$ (Newton and Coulomb laws). The power radiated by a black body scales with the fourth power of the temperature, $\alpha = 4$ (Stefan–Boltzmann law). The frequency of occurrence of a word is inversely proportional to its rank, $\alpha = -1$ (Zipf-Mandelbrot law). The list goes on and on. Scaling laws are ubiquitous but they are usually studied in isolation. Their apparent simplicity is often a consequence of the narrowness of the observational range. When data are gathered more broadly any scaling law is

[a] *Université Paris Cité, CNRS, Institut Jacques Monod, F-75013 Paris, France. E-mail: marc-antoine.fardin@ijm.fr*
[b] *Institut de Biologie Paris Seine, UMR 8263, Sorbonne Université, 7 quai Saint Bernard, 75005 Paris, France*
[c] *Department of Chemical Engineering, University of Illinois Chicago, Chicago, Illinois 60607, USA*
† The Academy of Bradylogists.

 This journal is © The Royal Society of Chemistry 2026

Published on 21 November 2025. Downloaded on 2/9/2026 5:09:59 PM.

bound to meet its demise. This statement has been verified time and time again by experiments. What we will show is that the eventual breakdown of a power law is actually a necessity if the associated phenomenon is to be independent of our human imprint. We will show that two intersecting power laws are needed to find objective units, and three to find an objective base.

This article is accompanied by video lectures on Youtube (**https://www.youtube.com/@naturesnumbers**), and a website making the data freely available (**www.numbersnature.org/explosions/data/trinity**). Details on how to use this material are provided in SI.

Scaling laws

Scaling laws have been studied in a wide variety of contexts and the arguments we shall develop in this article can be generally applied. We will however restrict our examples to particularly visual scaling laws tracking the evolution of a size or distance d over time t:

$$d \simeq Kt^{\alpha} \tag{1}$$

Note that we use an approximate rather than strict equality, because actual data sets rarely perfectly match a power law.

In eqn (1) if $\alpha = 1$ then motion is uniform and K is a speed. If $\alpha = 2$, motion is uniformly accelerated and K is an acceleration. If $\alpha = \frac{1}{2}$, K may be called a 'sorptivity',[6] but one usually writes $d = (Dt)^{\frac{1}{2}}$, defining a 'coefficient of diffusion' or 'diffusivity' $D \equiv K^2$. This definition allows to deal with a kinematic quantity with integer exponents, since $[D] = \mathcal{L}^2 \cdot \mathcal{T}^{-1}$, but $[K] = \mathcal{L} \cdot \mathcal{T}^{-\frac{1}{2}}$ (brackets are used to give the dimensions of the enclosed quantity). Generally K is a kinematic quantity, *i.e.* depending solely on space and time, with $[K] = \mathcal{L} \cdot \mathcal{T}^{-\alpha}$.

One example of the kind of power law defined in eqn (1) is found in many textbooks on scaling and dimensional analysis: $d = Kt^{\frac{2}{5}}$, which describes the extension of a blast wave of radius d, a time t after detonation.[1,2] In that case, K has no standard name, but for future reference we may call $X \equiv K^5$ an 'explosivity',[7] with $[X] = \mathcal{L}^5 \cdot \mathcal{T}^{-2}$, defined in such a way as to have integer exponents (like the diffusivity when $\alpha = \frac{1}{2}$). This $\frac{2}{5}$ scaling law was famously derived by G. I. Taylor and used to analyze the footage of Trinity, the first atomic test.[5,8]

Fig. 1a provides pictures of the Trinity test in the first few milliseconds after detonation. A number of these images had been declassified in a report published in 1947 by J. E. Mack,[4] the head of the optical team for the Trinity test. Taylor also got access to a few more pictures through his connection to the British Ministry of Supply, including the picture at $t = 1.22$ ms in Fig. 1a.[5] During World War 2 Taylor had been involved in the

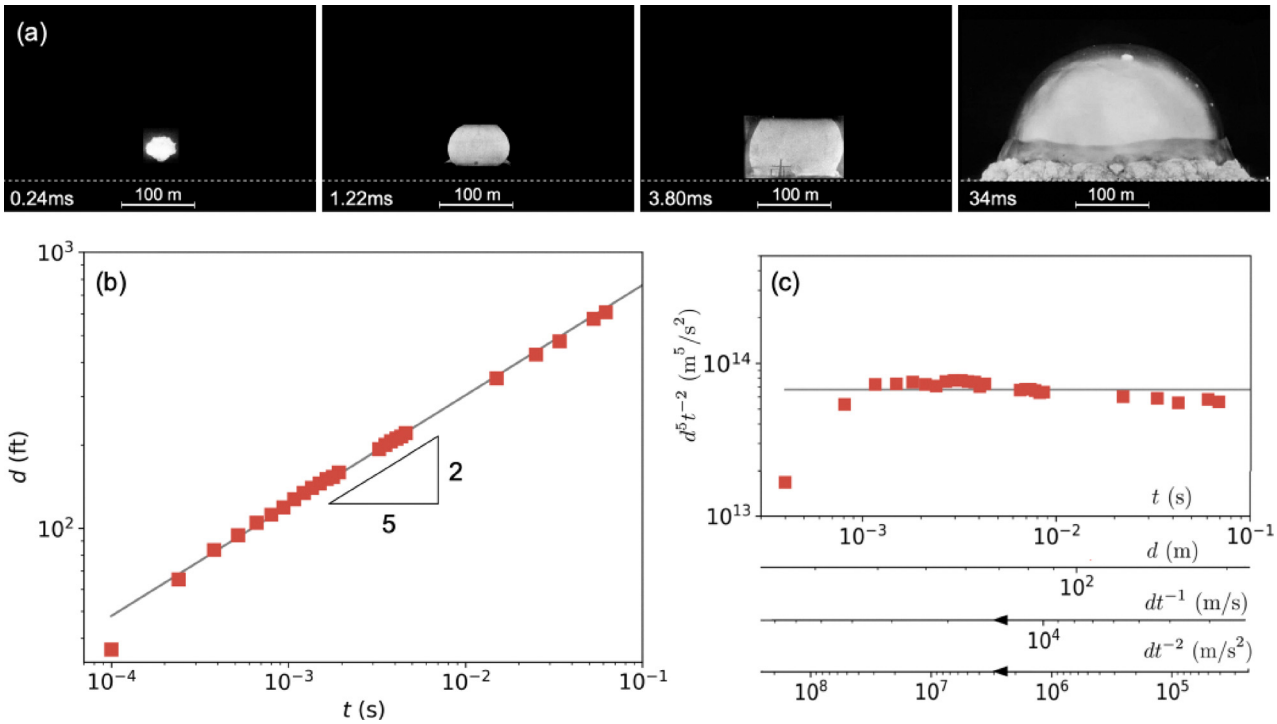

Fig. 1 Trinity: a paragon of scaling law. (a) Pictures of the nuclear test, taken by the optical team led by J. E. Mack,[3,4] and used by Taylor to analyze the kinematics of the explosion blast. Details and additional images are provided in SI and on a webpage (**https://www.numbersnature.org/explosions/data/trinity**) we created for the greater dispersion of these data (images courtesy of the Los Alamos National Laboratory). (b) Radius of the nuclear blast over time based on the images available to Taylor in 1950.[5] The grey line is $d = Kt^{\frac{2}{5}}$, with $K = 1913$ ft s$^{-\frac{2}{5}}$. (c) Replotting the data as an explosivity $\tilde{X} \equiv d^5/t^2$ *versus* time t, distance d, speed d/t, or acceleration d/t^2 – examples of the fact that the horizontal variable is indeterminate. The horizontal grey line is $X \equiv K^5$.

Published on 21 November 2025. Downloaded on 2/9/2026 5:09:59 PM.

Tube Alloys program, the secret British nuclear weapon project. After the Quebec Agreement on August 19th 1943, the British program was subsumed into the Manhattan Project, its American counterpart, and Taylor continued to play a major role.[9] In fact, Taylor was one of only two foreigners (the other being James Chadwick) in a very short list of ten "Distinguished Visitors" to be officially invited to the Trinity test in New Mexico.[9] In 1941 Taylor had predicted that the motion of a nuclear blast wave should follow a power law of the form $d = Kt^{\frac{2}{5}}$, and his prediction was confirmed by the Trinity test on July 16th 1945.[8] In 1950 Taylor was cleared to publish his own account in a couple of papers, a first paper on the theory behind such prediction,[8] and a second on the agreement between the prediction and the data from the Trinity test.[5]

Fig. 1b gives a logarithmic plot of the growth of the blast radius measured by Taylor on the pictures of the test, replotted from Taylor's second paper.[5] The agreement between the data and Taylor's scaling is indeed quite remarkable. On a logarithmic plot a power law appears as a straight line with a slope given by the exponent, here $\alpha = \frac{2}{5}$. The prefactor K sets the position of the line. In the case of Trinity, $K \simeq 1913$ ft s$^{-\frac{2}{5}}$. Taylor's impressive achievement was to connect this value to the yield of the explosion and to the density of the ambient medium (air in that case), providing a rational for this exotic exponent of $\frac{2}{5}$.[1,5,7,8] However, the underlying dimensional analysis is not the focus of this article. Our approach here is essentially phenomenological. We do not ask why the dynamics occur but how their existence shape our point of view.

Power laws, like Taylor's $\frac{2}{5}$ scaling, are generally understood to be 'scale-free',[10] since no preferred units of space nor time stand out. A power law is also said to be 'self-similar',[1] the dynamics following the same law regardless of scale, *i.e.* no matter how small or large the time t or radius d are. This nomenclature was introduced in the 1960s, in the wake of Benoit Mandelbrot's work on fractals,[11] and has remained popular in the literature on dimensional analysis.[1] However, both of these terms, 'scale-free' and 'self-similar', can be slightly misleading.

When space is measured in feet and time in seconds, then the value of K is around 1913. If we change the units, the value changes accordingly, for instance $K \simeq 583$ m s$^{-\frac{2}{5}}$. The fact that a power law is 'scale-free' does not mean that all units are equivalent, but that there is an infinity of equally good units. In this context, feet, meters and second are not "good units". As illustrated in the animated figures in SI (*cf.* SI Section SVII), if the coordinates (t_i, d_i) of any point along the power law are used as units, then the value of K in these units becomes trivial: $K \simeq 1 d_i/t_i^{\alpha}$. These units are "good units". Assuming d and t to be initially measured in any arbitrary units, this prevalence of some choices of units can be written in the following way:

$$\frac{d}{d_i} \simeq \left(\frac{t}{t_i}\right)^{\alpha} \tag{2}$$

Note that d/d_i and t/t_i can be read as d and t "in units of" d_i and t_i respectively. What remains arbitrary is the choice of point along the power law, *i.e.* the choice of a pair (t_i, d_i).

Units for a single axis

Technically, eqn (1) is often said to be scale-free or self-similar because $d/t^{\alpha} \simeq K$ is constant.[1,10] In the case of Taylor's scaling, $d/t^{\frac{2}{5}} \simeq K$. We are of course free to raise both sides to an identical power, in particular to a power of 5, and get $d^5/t^2 \simeq K^5$. The right-hand side is constant and is what we called an "explosivity".[7] Thus, the combination of variables in the left-hand side must also be a constant explosivity. Indeed, as shown in Fig. 1c, if d^5/t^2 is plotted against any other combination of variables, the data appear flat, and the value of the plateau is set by $X \equiv K^5$.

If d is plotted against t there is indeed no preferred units of space and time, any pair (t_i, d_i) is equally valid, and even any other units if we are allowing K to take non-trivial values, like $K \simeq 583$ m s$^{-\frac{2}{5}}$. However, the same dynamics can also be tracked using different variables. For instance, one might follow the speed of the shock front over time, or at various distances from ground zero. Measurements performed from different perspectives should be consistent, so in particular we should have $v \simeq Kt^{-\frac{3}{5}}$ and $v \simeq K^{\frac{5}{2}}d^{-\frac{3}{2}}$,[7] where $v \simeq d/t$ is the front speed (numerical factors are omitted; see SI Section SIII.A for details). The speed v, just like the size d and time t has no preferred scale. However, if instead we use the new variable $\tilde{X} \equiv d^5/t^2$, then this quantity is constant and it has a preferred scale, the unit of explosivity $X \equiv K^5$.

Power laws are apparently scale-free. The axes of the two primitive variables do not have preferred units. Nevertheless, there is always a way to combine the initial variables in such a way as to obtain a preferred unit for one axis, while the other axis remains indeterminate.[1,7] Basically, if $y = Kx^{\alpha}$, x and y do not have preferred units, but $(y/x^{\alpha})^{\gamma}$ has units K^{γ}, for any value of the free exponent γ. Such switch in perspective may seem a bit extravagant when performed on a single instance of a power law, but it becomes quite useful when comparing multiple examples. For instance, Fig. 2b gives the blast radii of a number of other atmospheric nuclear explosions,[4,5,16–18] conventional explosions,[13,14,19,20] an underwater explosion,[21] and laser-induced explosions.[12,22,23] A guide to the data is provided in SI. Some of these explosions are pictured in Fig. 2a. When these data are represented as the radius d *versus* the time t in conventional units, then the explosions appear quite different. The blasts go from microscopic to terrifying.

Since the scales of the explosions in Fig. 2b vary so much, it can be hard to believe that all these dynamics essentially display the same $\frac{2}{5}$ scaling derived by Taylor. Yet, as shown in Fig. 2c, if instead we plot the explosivity $\tilde{X} \equiv d^5/t^2$ for each explosion we indeed see that a portion of the data fall on plateaus, the ordinates of the plateaus are set by the values of K, *i.e.* the value of the explosivity scale $X \equiv K^5$ in each case. In Fig. 2c the explosivities of all examples are still measured in conventional units (m^5 s^{-2}). If instead we use the particular values of X as units in each case, all curves lie on the same horizontal (unity) plateau, as shown in Fig. 2d. Effectively, we have constructed a dimensionless number $N_1 \equiv \tilde{X}/X \equiv d^5/(t^2K^5)$, equal to unity as long as the dynamics follow Taylor's scaling (this number does not have a standard name, but we have

 This journal is © The Royal Society of Chemistry 2026

Published on 21 November 2025. Downloaded on 2/9/2026 5:09:59 PM.

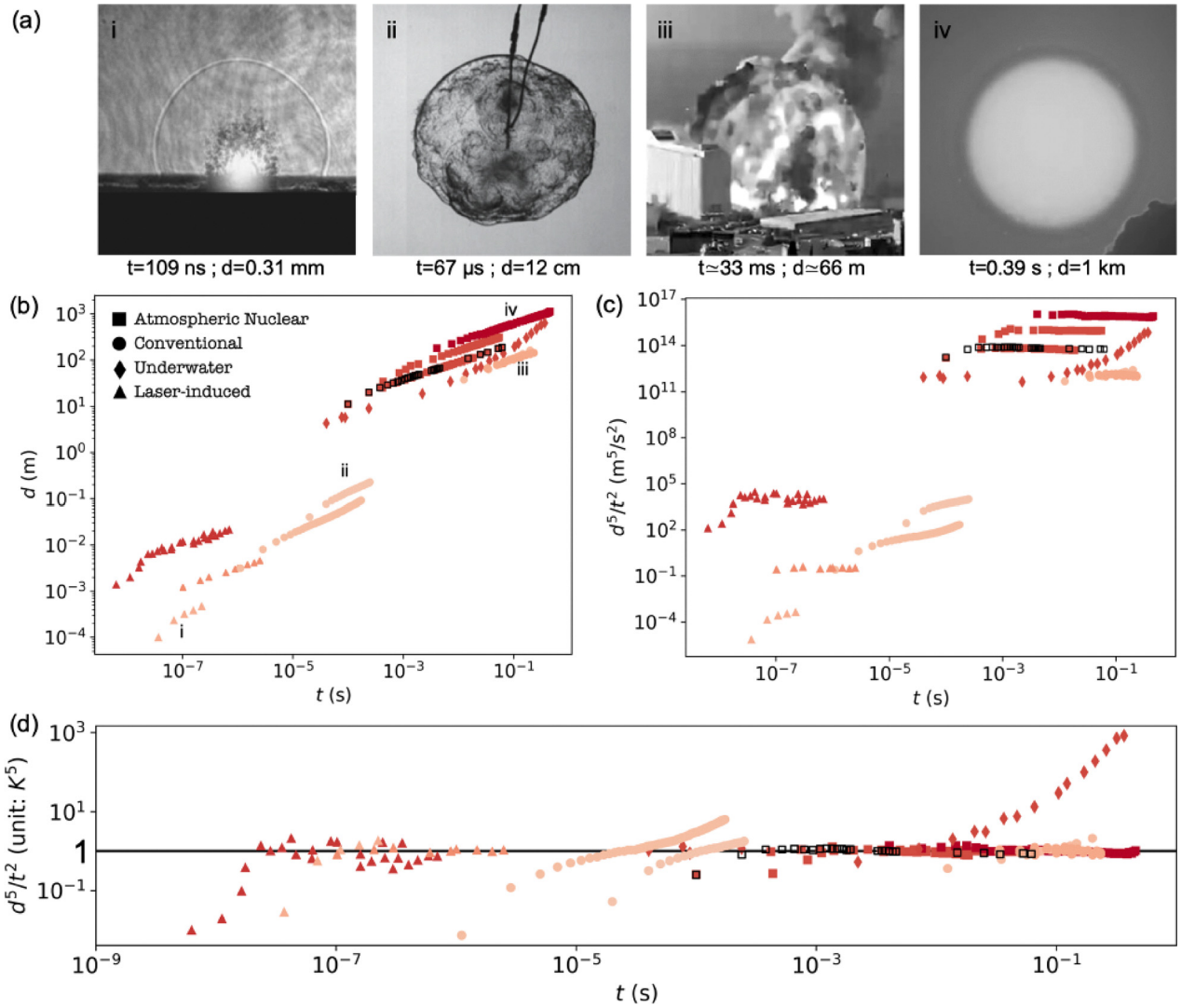

Fig. 2 Explosions across scales. (a) Pictures of explosions across scales. (i) Laser-induced explosion.[12] (ii) Explosion of a 1 gram charge of pentaerythritol tetranitrate.[13] (iii) 2020 Beirut explosion caused by 2.75 kilotons of ammonium nitrate.[14,15] (iv) Dominic Housatonic nuclear test (personal communication with G. Spriggs – Lawrence Livermore National Laboratory). Below each image the time since detonation t and the blast radius d are specified (**https://youtu.be/IZZ_IsyE_iE?si=aWDOslijsP2XB-SO**). (b) Blast radius over time for a number of nuclear (□: Trinity,[4,5] ■:[16–18]) and conventional (●:[13,14,19,20]) explosions in air, and underwater (♦:[21]), together with laser-induced explosions (▲:[12,22,23]). (c) Replotting the data as an explosivity $\tilde{X} \equiv d^5/t^2$ *versus* time. Most data sets show a plateau extending over a significant time range. The ordinate of each plateau gives the value of K^5 for that data set. (d) Using $X \equiv K^5$ as unit of explosivity, all plateaus align on $\tilde{X}/X \simeq 1$. A guide to the data and additional images are provided in SI and on this webpage (**https://www.numbersnature.org/explosions/2-beyond-trinity**). An animated version of panel b illustrating all data sets is given in SI (Fig. S2b.gif). The color code is explained later in the paper and quantified in Fig. 5. Note that the data sets on conventional explosions in pale pink only follow Taylor's regime over a very narrow time range, as will be explained later in the article.

recently proposed it be called the Taylor–Sedov number;[7] see SI Section SIII.A.1 for details). However, the horizontal axis in Fig. 2d still awaits a proper scale, and some portion of the data-whether in the initial, late, or both stages-departs from the plateaus where the curves no longer overlap. As we shall see now these two issues are connected and can be resolved.

Units for both axes

In his 1950 papers, Taylor considered the intermediate stage of the dynamics of a large explosion.[5,8] The pictures he used were just a subset of the ones taken by Mack's team.[3] Fig. 3a gives a more complete account of the dynamics, using data declassified in the 1980s[3] (we highly recommend reading this full report of immense historical value). The red squares outlined in black are the data points used by Taylor, replotted from Fig. 1. The other data points are from Mack's optical measurements, except for the squares with a central black dot, which were obtained from pressure measurements,[9] allowing to track the shock front beyond the point where it becomes transparent.[3,4] Although the shock front follows Taylor's scaling from a fraction of a millisecond to about 0.1 s after detonation, it eventually departs from it, decelerating progressively until it reaches the speed of sound, $c_s \simeq 344$ m s^{-1},

Published on 21 November 2025. Downloaded on 2/9/2026 5:09:59 PM.

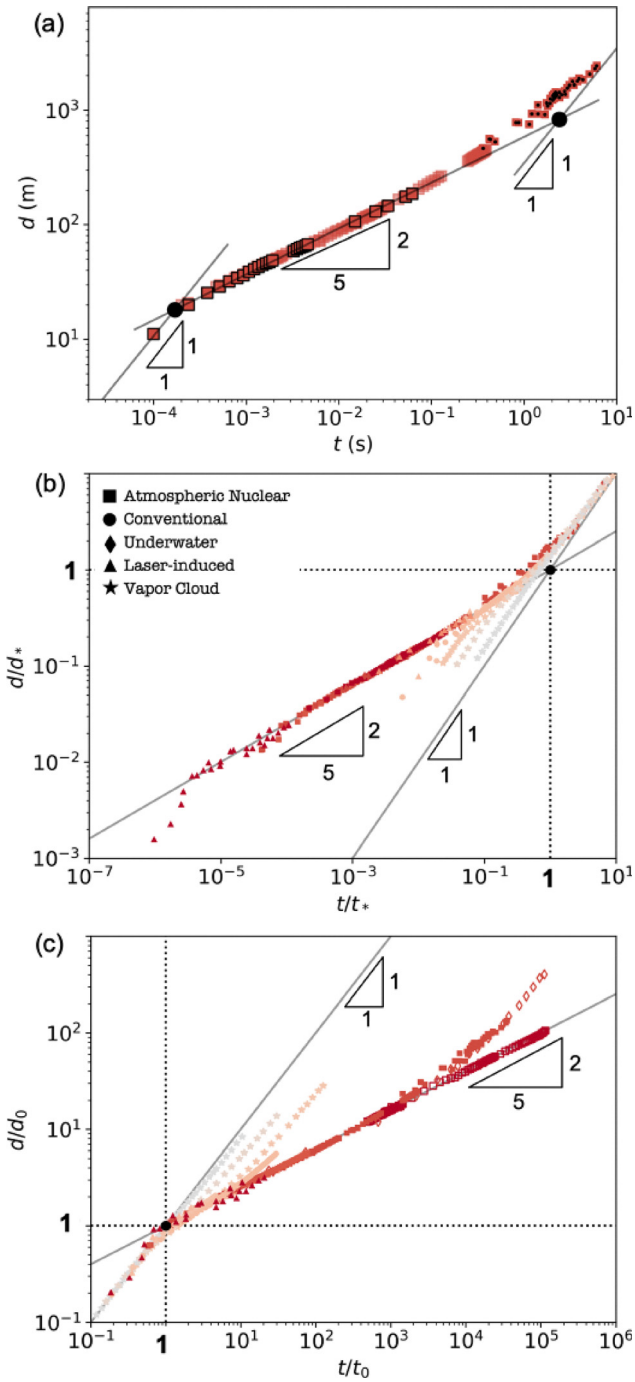

Fig. 3 Representing the dynamics of explosions with objective units. (a) Representation in standard units of an extended data set on the Trinity nuclear test, declassified in the 1980s. As a comparison, the black squares are the data used by Taylor.[5] Red squares are from optical measurement collected by Mack's team,[3] except those marked with a black dot, where the blast radius was inferred from pressure measurements.[9] (b) Data from Fig. 2 are replotted in Hopkinson–Cranz units, (t_*, d_*) defined in eqn (3) and (4). Also included are data on vapor cloud explosions (*), which were only provided in scaled form in the original paper.[24] (c) Objective units from the early dynamics of explosions, (t_0, d_0), defined in eqn (5) and (6). The grey lines are $d = Kt^{\frac{2}{5}}$, $d = c_0 t$, and $d = c_s t$. For data sets with hollow symbols the initial speed of the explosion is not directly measured but estimated from mechanical considerations (see SI Section SII.B for details). The color code is explained later in the paper and quantified in Fig. 5. Animated versions of panels b and c are given in SI to highlight each data set (Fig. S3b and c.gif). The files SI3b.gif and SI3c.gif provide animated transitions between Fig. 2b and 3b and c respectively, as explained in SI Section SVII.

denoted by the continuous line of slope 1 in Fig. 3a. This ultimate weakening of shocks had been understood since the beginning of the 20th century, notably thanks to studies by Bertram Hopkinson[25] and Carl Cranz,[26,27] the two scientists generally credited for understanding this transition.[28–30]

Hopkinson and Cranz realized that the blast of different explosions could be superposed if distance and time were measured in scaled units, which can be expressed using the speed of sound.[30] With the insight from Taylor,[5,8] we can understand the intermediate regime of the explosion as abiding to the scaling $d \simeq Kt^{\frac{2}{5}}$. As we previously saw, the front speed decreases over time as $v \simeq Kt^{-\frac{3}{5}}$. Eventually the speed of the front reaches the sound speed, $v(t_*) \simeq c_s$. The time t_* and radius d_* at which this transition occurs can be estimated by simply equating Taylor's regime, $d \simeq Kt^{\frac{2}{5}}$, with the late propagation at the speed of sound, $d \simeq c_s t$:

$$t_* \simeq \left(\frac{K}{c_s}\right)^{\frac{5}{3}} \tag{3}$$

$$d_* \simeq \frac{K^{\frac{5}{3}}}{c_s^{\frac{2}{3}}} \tag{4}$$

These units of space and time are often called the Hopkinson–Cranz units.[29] In contrast to the second and meter (or any absolute standards) these units depend solely on the characteristics of the dynamics. They are not set subjectively, but objectively, by the phenomenon at play.

Because the data eventually depart from Taylor's scaling, we acquire units for both space and time. Single power laws, $d \simeq Kt^{\frac{2}{5}}$ or $d \simeq c_s t$, do not have preferred scales. More precisely, for each power law taken separately, any couple of coordinates (t_i, d_i) on the power law provides equally valid units. However, when we now have two intersecting power laws, their point of intersection, here (t_*, d_*), provides a unique pair of units, a special point of view, common to both regimes.

For any explosion depicted in Fig. 2, we can compute the values of the associated Hopkinson–Cranz units, based on the measured explosivity and on the speed of sound in the medium (air, water, and some rarefied gases-see SI Section SVIII for details). For tiny laser-induced explosions, the Hopkinson–Cranz point may occur after just a few microseconds and for distances in the millimeter or centimeter range.[12,22] At the other end, a nuclear explosion like Dominic Housatonic has $t_* \simeq 20$ s and $d_* \simeq 5$ km (values of t_* and d_* are tabulated for all data sets in SI Table SV). Although these explosions may seem to have very different scales when measured with absolute but subjective units, their similarity is manifest once represented in relative but objective units. As shown in Fig. 3b, when the dynamics of small and large explosions are plotted in the Hopkinson–Cranz units, they largely overlap.

Note that the scaled units t/t_* and d/d_* are dimensionless numbers, and they can be connected to N_1 and to $N_2 \equiv (d/t)/c_s$, the Mach number associated with the late regime. As shown in SI Fig. S4b, the data can then be plotted as N_1 *vs.* N_2.

 This journal is © The Royal Society of Chemistry 2026

Published on 21 November 2025. Downloaded on 2/9/2026 5:09:59 PM.

Nevertheless, the same portions of the data overlap as in Fig. 3b, the same portion does not, and it is now time to address this point.

Competing units

Taylor was well aware that the $\frac{2}{5}$ scaling could only apply to the intermediate range of explosions.[5,8] He knew that at later times the shock would weaken sufficiently as to be almost indistinguishable from a sound wave, and he also knew that at very short time his scaling would fail. Indeed, we have seen that if the blast radius follows $d \simeq Kt^{\frac{2}{5}}$, then its speed follows $v \simeq Kt^{-\frac{3}{5}}$. The speed would seem to diverge at the instant of detonation. This is, of course, not the case in practice because at very short time the dynamics are governed by the initial ejection speed of the explosion, which we may call c_0.[31] Initially, the explosion front follows a third power law, $d \simeq c_0 t$. The various departures from Taylor's regime at short time seen in the figures capture this initial phase. In this initial phase, the impeding factor is usually the inertia of the ejected mass, but as for the previously discussed regimes, the mechanics are not in focus here (see SI Section SII.B.1 for details).

In the same way that we computed the crossover between Taylor's regime and the regime of sound propagation, we can now obtain the point of intersection between Taylor's regime and the initial regime at constant ejection speed:

$$t_0 \simeq \left(\frac{K}{c_0}\right)^{\frac{5}{3}} \tag{5}$$

$$d_0 \simeq \frac{K^{\frac{5}{3}}}{c_0^{\frac{2}{3}}} \tag{6}$$

This transition seems to have first been studied in the context of nuclear weapons development, in particular by the team led by Hans Bethe,[31] which included some famous members, like John von Neumann, and an infamous one, Klaus Fuchs (a notable atomic spy; see 2nd season of the BBC series "The Bomb"; https://www.bbc.co.uk/programmes/p08llv8n). This crossover is also discussed quite clearly in the literature on supernovae.[32,33] In this context, the initial ejection regime can last for centuries.

In Fig. 3b we had chosen to rescale the dynamics in such a way as to overlap the intermediate and late stages of the dynamics. Data sets with enough time resolution to capture the initial stage would not overlap. Instead, we can use the units (t_0, d_0) obtained from the early crossover to rescale the plot. Fig. 3c gives the result of such approach. Note that as done in SI Fig. S4b for the late crossover, we could tilt this scaled plot by using N_1 and $N_0 \equiv (d/t)/c_0$ (SI Fig. S4a). Either way, now the initial and intermediate regimes overlap but the late regimes do not. We have three consecutive regimes but it seems that we cannot rescale all of them at once. It is like having a short blanket on a cold night: pull it over your head and your feet get cold, cover your feet and your neck gets cold! Let now see how to knit a blanket with the perfect size to cover the three regimes of the dynamics.

A special number

With N_0, N_1 and N_2 we introduced three dimensionless numbers, which we may call "simple".[7] Each one of these numbers depends on a combination of the primitive variables, d and t, and on the kinematic constant of one of the three regimes, respectively, the initial speed c_0, Taylor's prefactor K, and the speed of sound c_s. Scaled variables, t/t_* and d/d_*, or t/t_0 and d/d_0 are more composite kinds of numbers, depending respectively on N_1 and N_2, or N_0 and N_1 (see SI Section SIV.A). These dimensionless numbers are still dependent on the variables d and t. There is, however, a special kind of dimensionless number depending solely on the parameters:

$$\mathcal{N} \equiv \frac{c_0}{c_s} \tag{7}$$

This number may be called the 'initial Mach number'[20] (also called the 'flame Mach number' for vapor cloud explosions[24]). For each explosion this number is a constant, and its value has been surreptitiously used as a color code in all figures. As seen in Fig. 3c for the units (t_0, d_0), and in Fig. 3b for the units (t_*, d_*), the non-overlapping part of the data produce a series of parallel curves with a darker shade of red the further they are from the origin (an illustration is provided in SI Fig. S6). Indeed, dark shades of red encode large values of $\mathcal{N}$, and we have $t_*/t_0 \simeq \mathcal{N}^{\frac{5}{3}}$, and $d_*/d_0 \simeq \mathcal{N}^{\frac{2}{3}}$. More broadly, the left-out regime in each system of units can be expressed using the number $\mathcal{N}$:

$$d \simeq c_0 t \leftrightarrow \frac{d}{d_*} \simeq \mathcal{N}\frac{t}{t_*} \tag{8}$$

$$d \simeq c_s t \leftrightarrow \frac{d}{d_0} \simeq \mathcal{N}^{-1}\frac{t}{t_0} \tag{9}$$

Solely rescaling the units does not allow the overlap of the three consecutive regimes at once. The two regimes going through the point of unit coordinates will overlap, but not the third regime. However, the prefactors of this third regime are set by the value of $\mathcal{N}$, and a complete overlap can be achieved if the importance of this number is fully acknowledged.

A new base for counting

In physics the term "order of magnitude" is often thrown around a bit loosely. Implicitly it is usually assumed that an order of magnitude is a decade, so two quantities separated by an order of magnitude will roughly differ by a factor of 10. How many decades a power law extends over is routinely used as a criterion to assess its worth. One may, for instance, say that Taylor's scaling is quite strong because it extends over almost three decades in time and over one in space. Ten is almost universally accepted as the base for counting, and indeed all logs we have used in the figures so far where logs in base 10.

Published on 21 November 2025. Downloaded on 2/9/2026 5:09:59 PM.

Nevertheless, this 10 is simply a convention, just like the meter or the second.

When we are dealing with a single power law, we have seen that the dynamics are scale-free, in the sense that no preferred units stand out. In the same way, a scaling law is also base-free. The choice of base for the log is completely arbitrary and so the meaning of an "order of magnitude" can be adjusted at will. This freedom is not lifted by the addition of a second intersecting power law, but by considering a third. In that case we have seen that a special kind of dimensionless number emerges, $\mathcal{N}$. The value of this number changes from one explosion to another, based on the values of the ejection and sound speeds. However, in every explosion, $\mathcal{N}$ plays the same role. It sets the coordinates of the crossover and the prefactors of the power laws. The number 10 was arbitrary, bound to our subjective choices. In contrast, $\mathcal{N}$ is an objective number set by the dynamics. The number $\mathcal{N}$ provides an objective base, or 'radix'. Indeed, when this number is used as a base for our logs, we can finally overlap all three regimes, as shown in Fig. 5a. In effect, Fig. 5a represents $\log_{\mathcal{N}}(d/d_*)$ *vs.* $\log_{\mathcal{N}}(t/t_*)$. SI Fig. S6 and S7 summarizes the whole route from subjective units and base to the more objective representation of Fig. 5a.

On a plot with objective units and base, choosing the origin to be at (t_0, d_0) or (t_*, d_*) does not affect the appearance of the plot, it solely shifts the coordinates (Compare SI Fig. S6c-i, ii and S7c-i, ii). For all curves, the full time range of Taylor's regime is always equal to $\frac{5}{3}$ "orders of magnitude" in base $\mathcal{N}$, and $\frac{2}{3}$ orders of magnitude in space, since $t_*/t_0 \simeq \mathcal{N}^{\frac{5}{3}}$, and $d_*/d_0 \simeq \mathcal{N}^{\frac{2}{3}}$ (top and right scale in Fig. 5a). If these fractions are unsettling, one may prefer to use the radix $R \equiv \mathcal{N}^{\frac{1}{3}}$ to get 2 orders of magnitude in space and 5 in time (bottom and left scale in Fig. 5a).

Duality

All explosions we have discussed so far were detonations: the initial ejection speed was always greater than the sound speed, so $\mathcal{N} > 1$. The converse is also possible. In that case, one speaks of deflagrations. As is apparent in Fig. 3b or c, the extent of Taylor's regime shrinks as $\mathcal{N}$ decreases toward unity. For deflagrations, when $\mathcal{N} < 1$, this regime is not expected to be present. This progressive disappearance is quite clear in the data on conventional explosions,[13,20] or on vapor cloud explosions[24] (pale pink data sets in the figures).

The blue path in Fig. 5a sketches what can be expected for deflagrations. The front proceeds at the constant ejection (or flame) speed. However, deflagrations are often affected by additional mechanisms (gravity, friction, *etc.*), and so their dynamics may deviate from this template. We invite the reader to contact us to point us toward data sets on deflagration that could be included in a revised version of Fig. 5a.

Note that $\mathcal{N} = 1$ is of course a singular case, which is quite obvious in a logarithmic representation in base $\mathcal{N}$, as in Fig. 5a. For data sets with $\mathcal{N}$ just slightly above 1 the transitions from one regime to another tends to be stretched out and smoothed out (curves with pale shades). SI Fig. S10 shows the extent of such distortions in the case of the vapor cloud explosions,[24] which were included in Fig. 3b and c, but excluded from Fig. 5a, since $\mathcal{N} \simeq 1^+$. This stretching effect and the case $\mathcal{N} = 1$ go beyond the scope of this article.

The duality between $\mathcal{N} < 1$, and $\mathcal{N} > 1$ can be sketched in the case of explosions, but it can be revealed more clearly for a different example, a second demonstration of the radical scaling approach we are promoting here. Whenever we have two intersecting power laws we acquire objective units. Whenever we have a third power law we can build an objective base or 'radix', hence the term 'radical' scaling. This procedure is absolutely general, so let us apply it to a different context: the dynamics of pinching,[40–46] spreading[34] and coalescing droplets and bubbles.[35–39] (Data used in Fig. 4 and 5b are from these cited references). We recently had the opportunity to review this field,[47] where scaling approaches have a long tradition.[48] Nevertheless, we had not gone through the extra step of renormalizing the number base.

Just as in the case of explosions, we are considering three consecutive power laws. For pinching, the neck of the drop is tracked as a function of the duration before pinch-off, for spreading, the contact radius is tracked since the instant of contact, and for coalescence, the radius of contact between the drops or bubbles is tracked since the instant they first touched.[47] In these three setups, for drops and for bubbles, a number of experiments have progressively evidenced the possible existence of three consecutive regimes[47] (other paths are possible,[49,50] but they are not in focus here). At short time, the trajectory is linear, $d \simeq c_v t$, then a power law of the form $d \simeq K_i t^{\frac{2}{3}}$ is observed, until the variable size d eventually reaches its maximum, set by the droplet or bubble size, $d \simeq D$. Experiments rarely have enough resolution to capture the three regimes, but their existence is inferred by piecing together multiple experiments.[47] In the case of explosions, the initial and final regimes were linear, hence parallel in a logarithmic plot. Thus we only had two points of intersection, with coordinates (t_0, d_0) and (t_*, d_*). Since the three regimes now have different slopes ($\frac{2}{3} \neq 1 \neq 0$), we have three points of intersection:

$$d_1 \simeq c_v t_1 \simeq K_i t_1^{\frac{2}{3}} \rightarrow t_1 \simeq \left(\frac{K_i}{c_v}\right)^3;\ d_1 \simeq \frac{K_i^3}{c_v^2} \tag{10}$$

$$d_2 \simeq D \simeq c_v t_2 \rightarrow t_2 \simeq \frac{D}{c_v};\ d_2 \simeq D \tag{11}$$

$$d_3 \simeq D \simeq K_i t_3^{\frac{2}{3}} \rightarrow t_3 \simeq \left(\frac{D}{K_i}\right)^{\frac{3}{2}};\ d_3 \simeq D \tag{12}$$

The first pair of coordinates provides what we have called the Ohnesorge units.[47] The two other pairs respectively correspond to what are usually called the visco-capillary and inertio-capillary units,[47] due to the mechanical underpinning of the constants K_i and c_v (see SI Section SII.B.2 for details).

 This journal is © The Royal Society of Chemistry 2026

Published on 21 November 2025. Downloaded on 2/9/2026 5:09:59 PM.

As seen in Fig. 4a, when plotted in standard units and with the traditional base 10, experiments on pinching, spreading, and coalescence crisscross each other in a tremendous mess. By choosing one of the three objective systems of units only two out of three regimes can be overlapped, as shown in Fig. 4b–d. The full overlap is reached by rescaling the base. As in the case of explosions, the kinematic parameters can be combined to obtain a dimensionless number. Now we have:

$$\mathcal{N} \equiv \frac{c_v D^{\frac{1}{2}}}{K_i^{\frac{3}{2}}} \tag{13}$$

Note that this number (like any dimensionless number) is defined *modulo* an overall power,[7] so for instance we could also use $\mathcal{N}^{-1}$, which is called the Ohnesorge number, or $\mathcal{N}^2$, which is called the Laplace number.[51] We choose the inverse of the Ohnesorge number (*i.e.* the square root of the Laplace number) as defined in eqn (13), in order to facilitate the comparison with the dynamics of explosions. The number $\mathcal{N}$ is a constant for each experiment, and just as with the initial Mach number for explosions, we can use $\mathcal{N}$ as our objective base. Fig. 5b gives the objective plot for these dynamics.

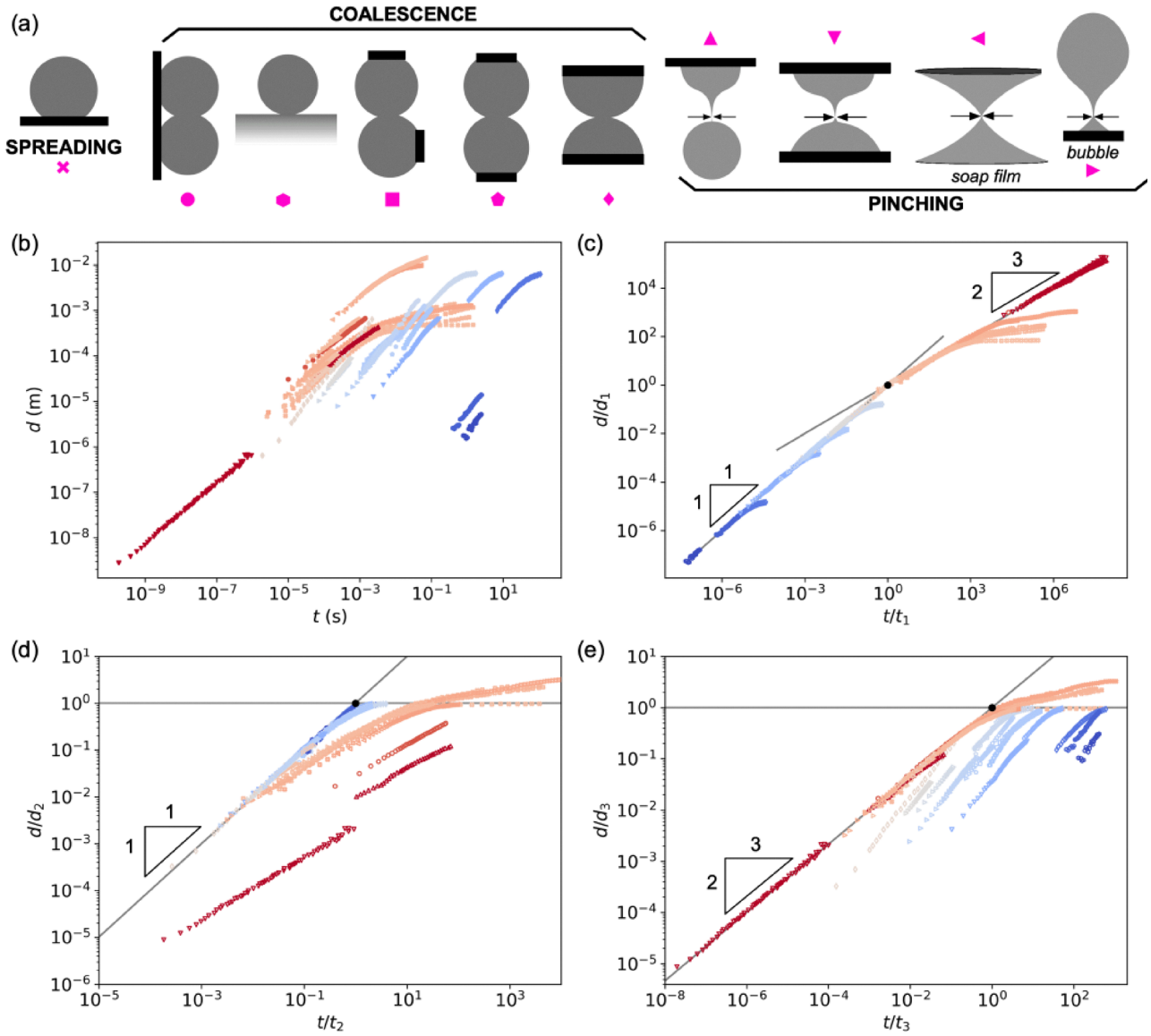

Fig. 4 Capillary dynamics of spreading,[34] coalescing,[35–39] and pinching droplets and bubbles,[40–46] represented with standard units or with the objective units provided by the crossovers. (a) Sketches of the various spreading, coalescence and pinching setups present in the figure. Each setup is associated with a symbol used for the data sets in panels b to e. (b) The data are represented in conventional units (1 s, 1 m). (c) The data are represented in Ohnesorge units (t_1, d_1), defined in eqn (10). (d) The data are represented in visco-capillary units (t_2, d_2), defined in eqn (11). (e) The data are represented in inertio-capillary units (t_3, d_3), defined in eqn (12). The continuous grey lines are $d \simeq c_v t$, $d \simeq K_i t^{\frac{2}{3}}$, and $d \simeq D$. The color code is explained later in the paper and quantified in Fig. 5. A guide to the data is provided in SI. Animated versions of each panel illustrating all data sets are given in SI (Fig. S4b–e.gif). The files SI4c–e.gif provide animated transitions between panel b and panels c, d and e respectively, as explained in SI Section SVII.

Published on 21 November 2025. Downloaded on 2/9/2026 5:09:59 PM.

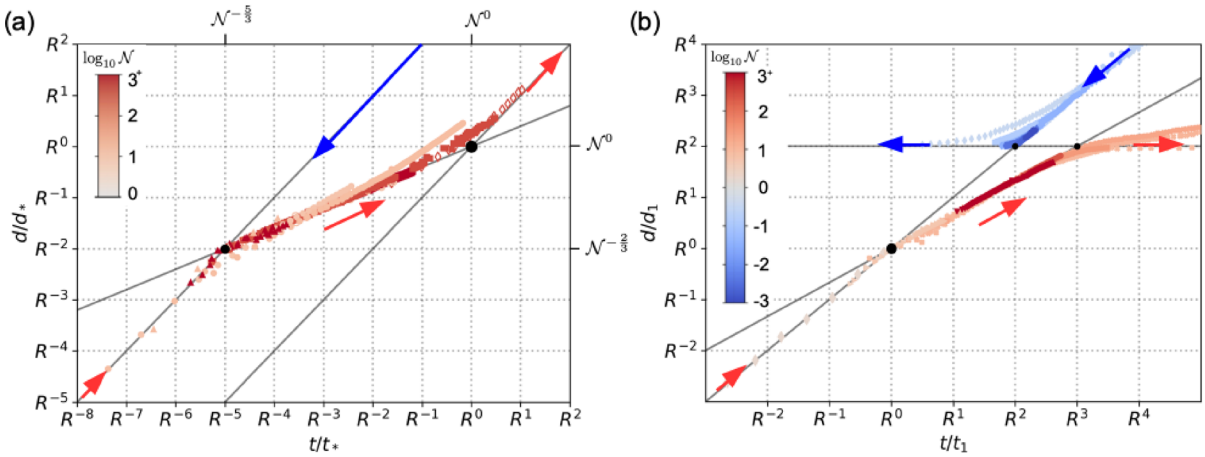

Fig. 5 Objective representations of the kinematics of explosions, and droplets and bubbles. (a) The explosion data introduced in Fig. 2 are plotted with objective units and an objective base. The units are (t_*, d_*) defined in eqn (3) and (4). The base is the initial Mach number $\mathcal{N} \equiv c_0/c_s$ (top and right scales), or $R \equiv \mathcal{N}^{\frac{1}{3}}$ (left and bottom), a radix chosen such that the points of intersections between the regimes occur at integer coordinates. Note that the data on vapor cloud explosions have been excluded from this plot. As discussed in SI Section SVI and Fig. S10 data sets with $\mathcal{N} \simeq 1$ are highly distorted with an objective base. (b) Capillary dynamics of pinching, spreading and coalescing droplets and bubbles[47] in objective units and base. The units are (t_1, d_1) defined in eqn (10). The base is the inverse of the Ohnesorge number, $R \equiv \mathcal{N} \equiv c_\nu D^{\frac{1}{2}} \Big/ K_i^{\frac{3}{2}}$. In both plots, dynamics with $\mathcal{N} < 1$ or $\mathcal{N} > 1$ proceed in opposite directions, since $\mathcal{N}^{n+1} > \mathcal{N}^n \leftrightarrow \mathcal{N} > 1$, a quite visual display of the duality of the dynamics. A guide to the data is provided in SI. Animated versions of each panel illustrating all data sets are given in SI (Fig. S5a and b.gif). The files SI5a.gif and SI5b.gif provide animated transitions respectively between Fig. 3b and panel a, and between Fig. 4c and panel b, as explained in SI Section SVII.

For these pinching, coalescence and spreading dynamics, the duality of the scaled plot is now clear. The succession of three regimes is only seen as long as $\mathcal{N} > 1$. When $\mathcal{N} < 1$ the linear regime at speed c_ν intersects the maximum size D before reaching the $\frac{2}{3}$ regime, which is now inaccessible. Usually one speaks of inertial dynamics when $\mathcal{N} > 1$ and of viscous dynamics when $\mathcal{N} < 1$.[47] Note that in Fig. 5, dynamics with $\mathcal{N} < 1$ or $\mathcal{N} > 1$ proceed in opposite directions, since $\mathcal{N}^{n+1} > \mathcal{N}^n \leftrightarrow \mathcal{N} > 1$, a quite visual display of the duality of the dynamics.

We are currently studying how this duality manifests itself in other examples and we encourage the readers to reanalyze the data they may be familiar with under this new light.

The pursuit of objectivity: radical scaling

Plotting a single power law requires a choice of units and a choice of base, choices that are made subjectively, solely guided by arbitrary conventions. In a plot like Fig. 1b the human presence is everywhere. Our feet are used to measure space, our hands to count, and the unit of time is barely less biased, a mixture of Egyptian and Babylonian fractions of the rotational period of our own planet. These choices are required to describe the phenomenon, but the phenomenon itself is expected to be independent of these choices. This independence can only be reconquered if the phenomenon is not as simple as initially thought, if the dynamics show at least three connected trends, rather than a single power law.

This inherent connection between the wondrous diversity of nature and the objective description of phenomena reveals a key insight: simplicity, as appealing as it may seem, often obscures the underlying richness of the world. A phenomenon that can be described by a single power law is inherently tied to the subjective choices of the observer—choices that impose our human scales and perspectives onto the data. In contrast, when we encounter a phenomenon characterized by multiple, connected power laws, we are granted the opportunity to strip away this human imprint. The units and bases used in our descriptions become dictated by the data themselves, reflecting the true nature of the phenomenon rather than our conventions.

It is important to distinguish, however, between the objective diversity of nature and mere complexity. Consider Fig. 2b or 4a, where multiple datasets, gathered under varying conditions, are plotted subjectively. The result is a tangled web of data points that seems overwhelmingly complex. This apparent complexity, however, is often a reflection of our arbitrary choices in units and base rather than the phenomenon itself. When these units and bases are determined objectively, as in Fig. 5, the data align in a more coherent and understandable pattern. By removing the subjective layers, we unveil a clearer, more interpretable representation of the underlying phenomena. What once appeared as a convoluted mess now reveals a pattern free from the distortions of human perspective.

Once they are stripped from our footprints and fingerprints, the data are ready to be interpreted. This interpretation does not rely on our measuring and reckoning conventions anymore: instead it usually invokes dimensions beyond those of the variables. For instance, when power laws are kinematic, relating space and time $d(t)$, like those we used as examples, then

 This journal is © The Royal Society of Chemistry 2026

Published on 21 November 2025. Downloaded on 2/9/2026 5:09:59 PM.

the interpretation may be mechanical, involving forces, pressures, *etc.*, quantities adding the dimension of mass to those of space and time. For instance, Taylor showed that the kinematic constant of the blast could be factorized as $K \simeq (E/\rho)^{\frac{1}{5}}$, where E is the explosion yield and ρ is the ambient density.[5,8] We recently reviewed this widespread decomposition of kinematic constants into pairs of mechanical parameters,[7] and have been publishing video lectures (**https://www.youtube.com/@naturesnumbers**) on how to address objective units and bases from such a mechanical point of view. What this article reveals is that a pair of mechanical quantities and its associated regime can only tell an incomplete story. A more complete scaling analysis should make an effort to identify three connected power laws, not just one, and this would require a minimum number of four mechanical factors. We will address these questions of mechanical combinatorics in a future article.

Conflicts of interest

There are no conflicts to declare.

Data availability

The data supporting this article have been included as part of the supplementary information (SI). See DOI: **https://doi.org/10.1039/d5sm00996k**.

Acknowledgements

M. H. thanks i-Bio funding. We thank N. Nikolova for her input on the manuscript. We thank G. McKinley, G. Spriggs, T. Wei and C. Aouad for enlightening discussions about drops, bubbles and explosions. We are grateful to A. Part (Atomic Heritage Foundation, National Museum of Nuclear Science & History) and A. Carr (Los Alamos National Lab.) for their help in collecting material about the Trinity test. Finally, we acknowledge the joyful atmosphere of the Ladoux-Mège lab, the stimulating haven that made this project possible.

References

1 G. I. Barenblatt, *Scaling*, Cambridge University Press, 2003.
2 J. G. Santiago, *A First Course in Dimensional Analysis: Simplifying Complex Phenomena Using Physical Insight*, MIT Press, 2019.
3 J. Mack, Tech. Rep., 1946.
4 J. E. Mack, Tech. Rep., 1947.
5 G. I. Taylor, *Proc. R. Soc. London, Ser. A*, 1950, **201**, 175.
6 J. R. Philip, *Soil Sci.*, 1957, **84**, 257.
7 M. A. Fardin, M. Hautefeuille and V. Sharma, *Soft Matter*, 2024, **20**, 5475.
8 G. I. Taylor, *Proc. R. Soc. London, Ser. A*, 1950, **201**, 159.
9 K. T. Bainbridge, Tech. Rep., 1976.
10 A.-L. Barabási, *Science*, 2009, **325**, 412.
11 B. Mandelbrot, *Fractals: form, chance and dimension*, San Francisco, Freeman, 1977.
12 C. Porneala and D. A. Willis, *Appl. Phys. Lett.*, 2006, **89**, 211121.
13 M. J. Hargather and G. S. Settles, *Shock Waves*, 2007, **17**, 215.
14 C. Aouad, W. Chemissany, P. Mazzali, Y. Temsah and A. Jahami, *Shock Waves*, 2021, **31**, 813.
15 S. Rigby, *Fire and Blast Information Group Technical Newsletter*, 2021, pp. 18–25.
16 P. O'Connell, Tech. Rep., Edgerton, Germeshausen & Grier Inc., No. B-30, 1957.
17 D. T. Schmitt, *Position and volume estimation of atmospheric nuclear detonations from video reconstruction*, Air Force Institute of Technology, 2016.
18 J. Nguyen, *Tech. Rep.*, Lawrence Livermore National Lab., Livermore, CA, 2017.
19 C. Kingery, J. Keefer and J. Day, *Tech. Rep.*, Army Ballistic Research Lab, Aberdeen Proving Ground, MD, 1962.
20 H. Kleine, *Eur. Phys. J.: Spec. Top.*, 2010, **182**, 3.
21 F. Porzel, *Tech. Rep.*, IIT Research Inst., Chicago, IL (USA), 1957.
22 M. Gatti, V. Palleschi, A. Salvetti, D. Singh and M. Vaselli, *Opt. Commun.*, 1988, **69**, 141.
23 J. Grun, J. Stamper, C. Manka, J. Resnick, R. Burris, J. Crawford and B. Ripin, *Phys. Rev. Lett.*, 1991, **66**, 2738.
24 M. Tang and Q. Baker, *Process Saf. Prog.*, 1999, **18**, 235.
25 B. Hopkinson, British Ordnance Board Minutes 13565, 1915.
26 C. Cranz, *Lehrbuch der ballistik, II band*, 1926.
27 P. W. Fuller, *26th International Congress on High-Speed Photography and Photonics*, SPIE, 2005, vol. 5580, pp. 250–260.
28 R. G. Sachs, *Tech. Rep.*, Army Ballistic Research Lab Aberdeen, 1944.
29 P. S. Westine, F. T. Dodge and W. Baker, *Similarity methods in engineering dynamics: theory and practice of scale modeling*, Elsevier, 2012.
30 T. Wei and M. J. Hargather, *Shock Waves*, 2021, **31**, 231.
31 H. A. Bethe, K. Fuchs, J. O. Hirschfelder, J. L. Magee, R. Peieris and J. von Neumann, Tech. Rep., 1947.
32 D. F. Cioffi, C. F. McKee and E. Bertschinger, *Astrophys. J.*, 1988, **334**, 252.
33 J. K. Truelove and C. F. McKee, *Astrophys. J., Suppl. Ser.*, 1999, **120**, 299.
34 A. Eddi, K. G. Winkels and J. H. Snoeijer, *Phys. Fluids*, 2013, **25**, 013102.
35 W. Yao, H. Maris, P. Pennington and G. Seidel, *Phys. Rev. E: Stat., Nonlinear, Soft Matter Phys.*, 2005, **71**, 016309.
36 M. M. Rahman, W. Lee, A. Iyer and S. J. Williams, *Phys. Fluids*, 2019, **31**, 012104.
37 D. G. Aarts, H. N. Lekkerkerker, H. Guo, G. H. Wegdam and D. Bonn, *Phys. Rev. Lett.*, 2005, **95**, 164503.
38 D. G. Aarts and H. N. Lekkerkerker, *J. Fluid Mech.*, 2008, **606**, 275.
39 J. D. Paulsen, J. C. Burton and S. R. Nagel, *Phys. Rev. Lett.*, 2011, **106**, 114501.

40 Y.-J. Chen and P. Steen, *J. Fluid Mech.*, 1997, **341**, 245.
41 G. H. McKinley and A. Tripathi, *J. Rheol.*, 2000, **44**, 653.
42 A. U. Chen, P. K. Notz and O. A. Basaran, *Phys. Rev. Lett.*, 2002, **88**, 174501.
43 J. Burton, J. Rutledge and P. Taborek, *Phys. Rev. Lett.*, 2004, **92**, 244505.
44 J. Burton, R. Waldrep and P. Taborek, *Phys. Rev. Lett.*, 2005, **94**, 184502.
45 R. Bolanos-Jiménez, A. Sevilla, C. Martnez-Bazán, D. Van Der Meer and J. Gordillo, *Phys. Fluids*, 2009, **21**, 072103.
46 R. E. Goldstein, H. K. Moffatt, A. I. Pesci and R. L. Ricca, *Proc. Natl. Acad. Sci. U. S. A.*, 2010, **107**, 21979.
47 M. A. Fardin, M. Hautefeuille and V. Sharma, *Soft Matter*, 2022, **18**, 3291.
48 P. G. de Gennes, *Rev. Mod. Phys.*, 1985, **57**, 827.
49 X. Xia, C. He and P. Zhang, *Proc. Natl. Acad. Sci. U. S. A.*, 2019, **116**, 23467.
50 J. Eggers, J. E. Sprittles and J. H. Snoeijer, *Annu. Rev. Fluid Mech.*, 2024, **57**, 61–87.
51 G. H. McKinley and M. Renardy, *Phys. Fluids*, 2011, **23**, 127101.

Published on 21 November 2025. Downloaded on 2/9/2026 5:09:59 PM.

 This journal is © The Royal Society of Chemistry 2026